

Preparation and characterization of activated carbon from *Typha orientalis* leaves

S. M. Anisuzzaman · Collin G. Joseph · Wan Mohd Ashri Bin Wan Daud · Duduku Krishnaiah · Ho Sie Yee

Received: 17 September 2014 / Accepted: 27 November 2014 / Published online: 27 December 2014
© The Author(s) 2014. This article is published with open access at Springerlink.com

Abstract

Background In this study, activated carbon (AC) was prepared from *Typha orientalis* or commonly known as cattail leaves using physical and chemical activation phosphoric acid (H_3PO_4), as dehydrating agent. A two-stage process was used, i.e., semi-carbonization stage at 200 °C for 15 min as first stage followed by second stage activation, at 500 °C for 45 min. The precursor material with the impregnated agent was exposed straight away to semi-carbonization and activation temperature using a laboratory scale muffle furnace (Carbolite RHF 1500, England) under static condition in a self-generated atmosphere.

Electronic supplementary material The online version of this article (doi:10.1007/s40090-014-0027-3) contains supplementary material, which is available to authorized users.

S. M. Anisuzzaman (✉) · D. Krishnaiah
Chemical Engineering Programme, Faculty of Engineering,
Universiti Malaysia Sabah, 88400 Kota Kinabalu,
Sabah, Malaysia
e-mail: anis_zaman@ums.edu.my

D. Krishnaiah
e-mail: krishna@ums.edu.my

C. G. Joseph · H. S. Yee
Water Research Unit, Faculty of Science and Natural Resources,
Universiti Malaysia Sabah, 88400 Kota Kinabalu,
Sabah, Malaysia
e-mail: collin@ums.edu.my

H. S. Yee
e-mail: collin_msc@hotmail.com

W. M. A. B. W. Daud
Department of Chemical Engineering, Faculty of Engineering
Building, University of Malaya, 50603 Kuala Lumpur, Malaysia
e-mail: ashri@um.edu.my

Results The best condition in AC production was based on chemical activation which is AC2 with 2 M of H_3PO_4 . AC2 has the highest removal efficiency, 97.4 % in 4 ppm concentration of Pb(II) and percentage yield of 62.73 % could be reached. The pH of the AC was controlled in the range 5–6. From Fourier transform infrared spectroscopy, functional groups such as hydroxyl group, lactone group, and carboxyl group were obtained. These were clearly illustrated by scanning electron microscopy micrographs that porous structure was progressively developed with sponge-like structure.

Conclusions The Pb(II) adsorption results were best fitted in the Langmuir isotherm for equilibrium data while the adsorption kinetic fitted to the pseudo-second order model. The maximum Brunauer, Emmett and Teller surface area of the best produced AC was found to be around 1,238 m²/g. The maximum adsorption capacity was found to be 7.95 mg/g.

Keywords Activated carbon · *Typha orientalis* leaves · Adsorption · Isotherm · Kinetics

Background

Several common processes have been carried out to control the water pollution. There are filtration, biological methods, adsorption, electrolysis, and activated sludge. Among these processes, adsorption can be the most effective method for the removal of heavy metals from wastewater using suitable adsorbents. Previous studies showed that AC has been widely used as absorbent on the removal of heavy metal from waste stream. AC is considered a quite expensive adsorbent because it is derived from high-cost sources such as wood, coal, and coconut shell [1].

Therefore, many researchers nowadays are searching for an alternative and environmentally friendly way to produce the most cost-effective and cheapest adsorbent for economical wastewater treatment by testing variety of raw material ranging from industrial waste product to agricultural product.

Over the recent decade, environmental researchers and adsorption investigators have focused on the production of green adsorbent to remove the pollutants and control for competitive sustainable development [2, 3]. Currently, the literature survey indicates that very few articles have reported the use of cattail leaves as a potential precursor which can effectively adsorb the heavy metal contaminants in aqueous solution. *Typha orientalis* or commonly known as cattail is one of the most common aquatic plants. It is mainly composed of lignocelluloses which can be found in wetlands, margins of ponds, and lakes. Besides that, it provides excellent cover and nesting habitat for certain wildlife [4]. It is widely use for water treatment, treatment of soil contamination [5, 6] and also the removal of phosphorous and heavy metals [7]. It utilizes the solar energy effectively and spreads rapidly because their seeds are blown by the wind, then floats on the water's surface and by vegetative, they can also spread from underground rhizomes. Due to its ability to growth rapidly, a large amount of biomass is produced which can pollute the resource of the environment [4]. Thus, the abundance and existence of cattail encourage the research to produce AC from cattail leaves. According to previous studies, cattail biomass could be a reason to anaerobic digestion that results in biogas production [7]. It is also known as a perennial aquatic plant where they can grow abundantly in fresh water wetlands and can be used for wastewater treatment in constructed wetlands [8–10]. This plant can give a good development in adsorbent material due to its ability to absorb large quantity of nutrient and produce biomass which are at no cost needed [11].

This study was focused on preparation and characterization of AC prepared from cattail leaves using two-stage self-generated atmospheres in a laboratory scale Muffle Furnace and to evaluate the adsorption capacity of the prepared AC by adsorbing heavy metal such as Pb(II) ion in aqueous medium.

Methods

Experimental procedure

The cattail leaves were harvested from a pond in the University Malaysia Sabah (UMS) campus Kampung E, Sabah. These leaves were washed with tap water to remove the dirt. It was then dried under the sun for 5 days after

being cut into small pieces measuring ± 0.5 cm. The sample pieces were washed with distilled water for several times and dried it in an oven at 110 °C overnight. Then, the dry cattail sample was stored in the sealed container for experimentation. Impregnation of dry cattail pieces is done using different concentrations (0, 2, 4 and 6) of phosphoric acid (H_3PO_4) as dehydrating agent. These concentrations were prepared separately in each Erlenmeyer flask. Cattail samples (20 g/sample) inside the flask were soaked and shaken with the prepared H_3PO_4 solution in water bath shaker for 3 days with 70 rpm at 80 °C. The reason to soak and shake the sample is to ensure that the reagent absorbs into the raw material [12].

After impregnation process, samples were transferred into a Petri dish and dried at 110 °C for 24 h. Later, they were weighed, transferred to a clean crucible, covered with a lid and kept in a sealed container for further processing. A muffle furnace (Carbolite RHF 1500, England) was used for semi-carbonized and activation process. Before inserting samples into muffle furnace, the temperature of the muffle furnace was set to maintain at 200 °C. Then, each of the cattail samples undergone semi-carbonized for 15 min and the furnace temperature was adjusted to the desired activation temperature at 500 °C and the sample was activated for 45 min.

Then, the chemical AC was refluxed with distilled water for 3 h and this step was repeated for several times until a constant pH was observed. While for the physical activation of AC, it was refluxed with 0.1 M HNO_3 to remove heavy metal ions, tar, and ash. Then, it was followed by second step refluxed with distilled water for several times to remove the acid [13]. The AC was dried in an oven for 4 h at 105 °C. Then, the sample was analyzed for percentage of yield, ash, moisture content and pH. Fourier transforms infrared spectroscopy (FTIR) was used to study the surface functional group; scanning electron microscopy (SEM) was used to study morphological characterization and flame atomic absorption spectrophotometer (FAAS) was used for AC sample elements. The surface area of the particles was determined by Brunauer, Emmett and Teller (BET) apparatus.

Determination of percentage of yield

The percentage of yield can be obtained by taking initial mass of the impregnated sample divided by the final mass of sample at the end of activation process by the following equation:

$$\% \text{ of yield} = \frac{W_f}{W_i} \times 100 \% \quad (1)$$

where W_f is initial mass of the dry impregnated sample and W_i is the final mass of sample at the end of activation process.

Determination of ash content

Approximately, 1.0 g of sample weighed in a tarred weighing beaker and the dried sample was transferred into a tarred crucible. The sample ignited until it was completely burned using muffle furnace at 500 °C for 4 h and then it was cooled in desiccators. The weight loss is obtained and the ash content is calculated using equation as follows [14]:

$$\begin{aligned} & \% \text{ of ash content} \\ & = \frac{\text{Weight of sample after ash process} \times 100 \%}{\text{Weight of sample before ash process}} \quad (2) \end{aligned}$$

Determination of moisture content

According to Standardization and Industrial Research Institute Malaysia (SIRIM) method, 1.0 g of sample weighed in a tarred weighing beaker to the nearest 10 mg and placed in a drying oven for 2 h at 110 °C. The sample then cooled in desiccators and weighed immediately to prevent moisture absorption. Percentage of moisture content was determined as follows:

$$\begin{aligned} \% \text{ of moisture content} & = \frac{\text{Loss of weight} \times 100 \%}{\text{Weight of sample after drying}} \\ & \quad (3) \end{aligned}$$

Determination of pH

Approximately, 1.0 g of AC was put inside a 250-mL Erlenmeyer flask. Then, 100 mL of distilled water was poured inside the Erlenmeyer flask. The solution was heated for 5 min in gentle boiling condition. Later, the solution was cooled to room temperature and diluted with distilled water to 100 mL. Solution was stirred well and the pH was determined using pH meter (Mettler Toledo MC 226, Switzerland) [14].

Functional groups determination

Fourier transform infrared spectroscopy was used to study the surface functional group of the AC so that the chemical structure of the prepared AC can be determined. IR spectra were obtained with a type Spectrum 100 series FTIR spectrometer (Perkin Elmer Spectrum 100, USA) using the transformation of 20 scans with a spectral resolution of 4 cm^{-1} by attenuated total reflectance method. FTIR spectra were collected in the mid infrared region between 4,000 and 650 cm^{-1} . Spectra were acquired using air background correction.

Morphological characterization

SEM (JEOL JSM-5610LV, Japan) at 10 kV with a magnification of 3,000 \times was used to observe the porosity and

morphological surface of the prepared AC. Samples were mounted on self-adhesive carbon sticky tape and gold coated before imaging (JFC-1600 auto fine coater operated at 20 mA for 120 s, Japan).

Specific surface area and pore-distribution

The specific surface area and the pore-size distribution were determined from nitrogen isotherm at 77.3 K using Quanta chrome autosorb automated gas sorption instrument, USA. Prior to analysis, the adsorbents are out gassed for 12 h under vacuum at 110 °C. The specific surface area determines according to the BET method at the relative pressure at 33.5 atm.

Adsorption experiment

Adsorptions of single solute, Pb(II) onto prepared AC were carried out and the obtained equilibrium data were fitted to equilibrium models to evaluate the relative suitability of the prepared adsorbents. Then, the performance of the best AC was selected to evaluate and compare with the relative affinity for developing a selectivity order over a range of concentration.

Effect of time on Pb(II) adsorption

The study was carried out for different contact time at a fixed adsorbent dosage and initial concentration of Pb(II). To determine the exact concentration of adsorbate, a control sample was taken before get contact with the activated carbon. 0.1 g of dry fine AC was put into a 250-mL Erlenmeyer flask with 200 mL of Pb(II) stock solution. After that, the flask capped with parafilm and agitated for 45 min on an orbital bath shaker at room temperature. AC was transferred out and filtered during each 5 min of the contact time and kept in stoppered plastic bottles. After filtration, the filtrates are ready to be analyzed using FAAS (Perkin Elmer AAS 4100, USA) to determine the residual metal concentration. The above procedure was repeated using 0.1 g of AC2, AC3 and AC4.

Effect of initial concentration on Pb(II) adsorption

This study was carried out with varying initial concentration of Pb(II) at a fixed dosage of adsorbent (0.1 g). The concentrations used for the initial concentration were 4, 8, and 16 ppm. After that, 0.1 g of cattail AC1 was added into each Erlenmeyer flask and the mixture was shaken on an orbital shaker for 45 min. Subsequently, the mixtures were transferred out and filtered for FAAS analysis. The above procedure was repeated using 0.1 g of AC2, AC3 and AC4.



Effect of dosage of adsorbent on Pb(II) adsorption

Then, the performance of the best AC was selected to study the effect of dosage of adsorbent on Pb(II) adsorption. The experiment was carried out for different dosage of adsorbent at a fixed initial concentration of Pb(II). Three Erlenmeyer flasks filled with 200 mL of Pb(II) solution which represent different dosage of adsorbent, namely 0.1, 0.3, and 0.5 g were shaken on orbital shaker for 45 min. After that, the mixtures were transferred out and filtered for FAAS analysis.

Determination of Pb(II) concentration

The absorbance value of standard Pb(II) solutions, 4, 8, 12, 16, and 20 mg/L was measured by using FAAS. The absorbance was plotted against concentration to obtain the calibration graph. The mixtures that transferred out were then filtered using Advantech No. 9 filter paper and kept in stoppered plastic bottles. The absorbance was set to zero using distilled water as the blank prior to measurement. The final concentration of Pb(II) was then determined using FAAS. The percentage removal and the amount of Pb(II) adsorbed onto AC were calculated according to the following equations:

$$q = \frac{(C_0 - C_e)V}{m} \quad (5)$$

$$\% \text{ removal} = \frac{(C_0 - C_e) \times 100 \%}{C_0} \quad (6)$$

where q is the amount of Pb(II) adsorbed per gram of adsorbent (mg/g), C_0 is the initial Pb(II) concentration (mg/L), C_e is the concentration of Pb(II) at equilibrium with the solid phase (mg), V is volume of the working solution used (L), and m is mass of the adsorbent used (g).

Results and discussion

Percentage of yield

Table 1 shows the results of different parameters measured. It shows that the concentration of H_3PO_4 played a major role in the evaluation of prepared AC. Based on the data as shown in Table 1, percentage of yield increases from 39.22 to 73.10 %. The highest percentage yield represented by AC4 is 73.10 % while AC1 showed the lowest percentage yield of 39.22 %. It also shows that percentage of yield increases as the concentration of H_3PO_4 increases. This is because the chemical activator, H_3PO_4 , acts as a skin phosphate which can be used to protect the internal carbon structure and prevents the product from excessive burn-off [15]. There is a big percentage yield difference

between physical AC and chemical AC which can be observed from Table 1. Liu et al. [16] have done the similar research using H_3PO_4 as dehydrating agent in preparation of AC from bamboo. The reason for high percentage yield in chemical AC was due to the H_3PO_4 activation, which caused more potential sites to penetrate and occupy the activating agent. This enhances the pore opening and widening.

Ash content

Normally, the ash content of the AC is dependent on the ash content of the precursor. The ash is a non-carbon material, which is usually mineral additive that is not attached to the surface of the carbon. It can influence the adsorptive capacity of the prepared AC as it is linked directly to the pore structure of the AC. In other words, when the value of the ash content decreases, the efficiency and adsorptive capacity of the prepared AC increase. Based on the experimental results as shown in Table 1, the impregnated carbon with H_3PO_4 had more ash content compared to physical AC. The physical AC contained 3.20 % ash and the rest of the chemical AC had an increasing trend of ash content in the range of 4–6 %. By altering H_3PO_4 concentration, this could bring about very significant changes in the ash content of the prepared AC. This is due to some chemical remained in the AC after washing which contributed to the ash content in the AC [17]. Thus, these entrapped polyphosphates in the AC contribute to high ash content and lower the surface area on the final product as the concentration of H_3PO_4 increases [18].

Moisture content

The average moisture content of the AC samples was in the range 2–3 %. There is no significant change with the concentration of dehydrating agent applied. The moisture content in these samples may be attributed to the adsorption of moisture from the surrounding atmosphere after activation process, because almost all the moisture should be removed during the two-stage activation process at high temperature. Even though they might absorb moisture content from the surrounding, but it still appears dry. Lowering the moisture content results better in AC, because water vapors compete in adsorption process and fill the adsorption sites within the pores, thus reducing the efficiency of the AC [19].

pH value of the AC samples

Based on the data as shown in Table 1, prepared AC from impregnated cattail leaves with H_3PO_4 was acidic. Overall,

Table 1 Percentage of yield, ash content, moisture content, pH and its parameters

Sample	H ₃ PO ₄ concentration	Activation temperature and time	Percentage of yield (%)	Ash content (%)	Moisture content (%)	pH
AC1	0 M	500 °C, 45 min	39.22	3.20	2.50	6.32
AC2	2 M	500 °C, 45 min	62.73	4.49	2.20	6.18
AC3	4 M	500 °C, 45 min	71.83	5.09	2.91	5.76
AC4	6 M	500 °C, 45 min	73.10	5.19	2.70	5.32

the AC had a pH 5.00 and above. The pH value of the AC samples was obtained after the washing process, where the chemical AC prepared by two-stage self-generated atmosphere method was refluxed with distilled water for 3 h and this step was repeated for several times until a constant pH was observed. The physically activated AC was refluxed with 0.1 M HNO₃ to remove heavy metal ions, tar, and ash, then followed by second step refluxed with distilled water for several times to remove the acid [13]. The amount of HNO₃ solution as well as distilled water used in the washing process is not fixed for each sample. The purpose of washing is to remove residue and dust from the samples. Generally, pH of the AC influenced the surface chemistry and adsorption of various adsorbates that are sensitive to the pH changes. In this study, the pH of the final product was controlled during the washing process to ensure a neutral pH value.

Fourier transform infrared spectroscopy analysis

Fourier transform infrared spectroscopy was used to study the functional group and obtained information on the chemical structure of the prepared AC. The surface chemistry of an AC was determined by the type, quality, and bonding of functional group. Figure 1 shows the spectra of raw cattail leaves, physical AC (0 M) and chemical AC (2, 4, 6 M). In general, all the spectra almost showed the similar pattern and functional group due to the same precursor used. Based on the Fig. 1, there were no significant changes observed in spectra when varying the concentration of dehydrating agent. Similar spectra results have also been obtained for AC prepared from cattail leaves [20, 21]. A broad band located around 3,300–3,800 cm⁻¹ is typically attributed to the presence of hydroxyl group either aliphatic alcohol or phenol or even adsorbed water molecule. The band around 1,600–1,800 cm⁻¹ is possibly caused by the stretching vibration C=O in carboxyl, ketone, aldehyde, and lactone group. Stretching vibration at 1,400–1,600 cm⁻¹ corresponds to the aromatic ring or C=C bonding. Presence of this functional group indicates the formation of carbonyl-containing group and aromatization of the precursor [22]. While the band around 1,200 cm⁻¹ is typically represented

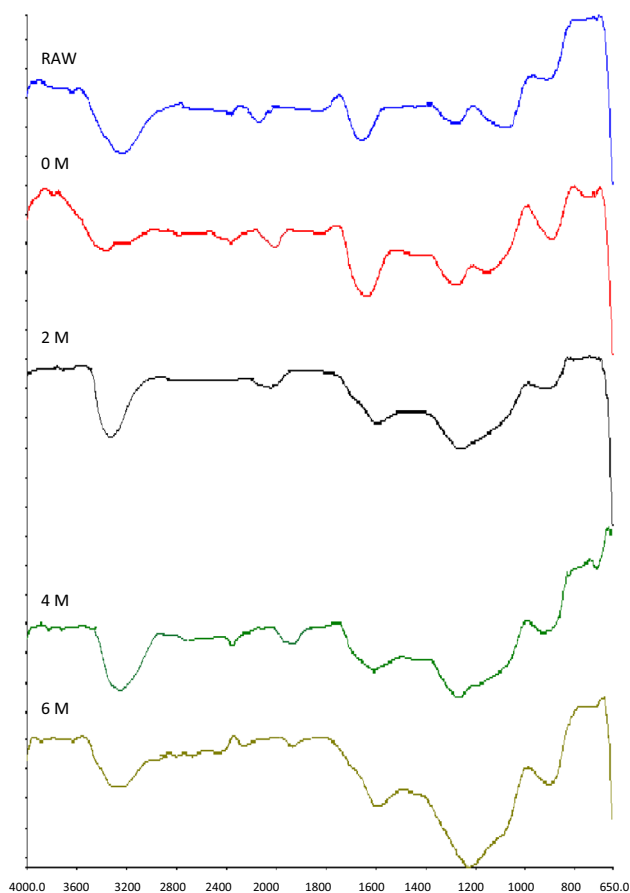


Fig. 1 FT-IR spectra of raw cattail leaves, physical AC (0 M) and chemical AC (2, 4, 6 M)

by the C–O group. In chemical activation involving the H₃PO₄, the chemical activator promotes depolymerization, dehydration, and redistribution of constituent biopolymer which causes the decomposition of the lignocellulosic material when it underwent pyrolysis. Thus, at low temperature the conversion of aliphatic to aromatic compound can be enhanced [23]. For the spectrum of chemically prepared AC, the band in the region 900–1,300 cm⁻¹ could be caused by the phosphorus-containing groups. The peak around 1,180–1,220 cm⁻¹ could be caused by the stretching of P=O bond in phosphate ester, O–C bond in P–O–C linkage, or P–OOH bond. According to Puziy et al. [24], presence of this band indicates the presence of phosphorus-

containing groups in the prepared AC. Table 2 presents the frequencies in the IR spectra and their respective possible band.

Textural characterization by scanning electron microscopy (SEM) analysis

The SEM was used to identify the porous structure and external surface of the AC. The size and distribution of the pores for the samples were prepared under different conditions as shown in micrograph from SEM. The development of the pore system in AC depends on the precursor sources and the manufacturing process. The average amount of pores greatly depends on the concentration of impregnation agent [25]. The scanning electron micrographs in Figs. 2, 3, 4, 5 and 6 show that the morphology of the pore increases from AC1 to AC2 as the impregnation concentration increases, and decreases for AC3 and AC4. The surface structures of the cattail leaves have dirt-covered and unclear pores as shown in Fig. 2a, b, whereas the surface structures of the AC1 have a cleaner and burnout pores with tunnel or honeycomb-like structures. The AC1 obtained from physical activation process showed the lowest pore amount as shown in Fig. 3a, b. The impregnation concentrations seemed to play an important role than activation process in determining the porosity. Figure 4a, b shows that progressive development of porosity takes place by producing agglomeration of pores as the impregnation concentration increases to 2 M H_3PO_4 . It is evident that based on the data from Pb(II) adsorptive capacity shows that AC2 has the highest percentage removal, 97.4 %. Thus, AC2 is preferable to be a high quality AC.

The chemically impregnated AC, AC3 (Fig. 5a, b) and AC4 (Fig. 6a, b) showed a negative trend of porosity development. It may be attributed to the damage of the morphological structure of the activated carbon. Besides that, these results are possible because some of the pores were clogged with H_3PO_4 even after undergoing washing process. The reaction of H_3PO_4 with the lignocellulosic material gave a burn-out sponge-like structure as shown in

Fig. 6a [13]. It displays the similar results and also shows the collapsed morphology structure [18, 26]. With excessive impregnation with H_3PO_4 , it might form an insulating layer which inhibits the activation process [27]. Besides, it was found that washing process played a crucial role for the development of pore in activated carbon. This is because after activation at high temperature, most of the chemical activator remains in the particle and intense washing eliminates the chemical. Thus, it produces more porous AC. However, polyphosphate that is being entrapped in AC appears in the form of ash content or gave the final product with acidic character [26]. Therefore, to ensure that the acid content is successfully removed from the AC, the washing process is repeated until a near neutral pH is obtained. The overall micrographs for AC2, AC3 and AC4 showed an irregular and heterogeneous surface morphology with moderately developed porous structure. The external surface of the AC is full of cavities and with irregular shape distributed. The formation of these cavities resulted from the evaporation of the dehydrating agent (H_3PO_4) during carbonization, leaving the space previously occupied by the reagent [28]. Chemical AC seems to be clearer and smoother compared to physical AC due to the removal of volatile compounds and impurities during the activation process [18].

Specific surface area and pore-distribution

Table 3 represents the porous and surface characteristics of AC2. The highest surface area and pore volume obtained from the Langmuir equation were $1,238.60 \text{ m}^2/\text{g}$ and $284.55 \text{ cm}^3/\text{g}$, respectively. Mesoporous volume was found to be 0.0462 from Brrett–Joyner–Halenda, Cranston, Inkley and Dollimore methods. The micropores' volume was relatively more compared to mesopores indicating that micropores contribute to the kinetics of adsorption.

Effect of contact time on Pb(II) adsorption

AC2 demonstrated the highest percentage removal of Pb(II) and it was found to be 97.4 %. The adsorption rate of Pb(II) is rapid in the early stage and then slows down as the contact time becomes longer. The adsorption of Pb(II) onto AC occurred in two stages: an initial rapid uptake due to the presence of vacant adsorption site on the AC, subsequent slow uptake due to diffusion of the Pb(II) onto the inner surface of cattail AC and the left over active site in the adsorbent is less available to be occupied [29]. Pb(II) exhibited a rapid adsorption by AC2 during the first 5 min with the percentage of removal, 84.0 %, and then followed by a slow adsorption process until 45 min with percentage removal of Pb(II) up to 97.4 %. Thus, the experimental sorption capacity at equilibrium q_e (mg/g) was determined

Table 2 Peak frequencies in the IR spectra and possible assignment of the band

Band position (cm^{-1})	Possible assignment
3,809, 3,788, 3,742, 3,713, 3,613	O–H stretching
2,361, 2,358, 2,356	CO_2 present in chamber
1,656, 1,636, 1,605, 1,592, 1,589	C=O stretching vibration
1,549, 1,462, 1,427	C=C stretching vibration
1,280, 1,273, 1,272, 1,263	C–O stretching vibration
1,158, 1,068, 932, 915, 902, 895, 828, 788, 755, 721, 713, 699	P=O stretching vibration



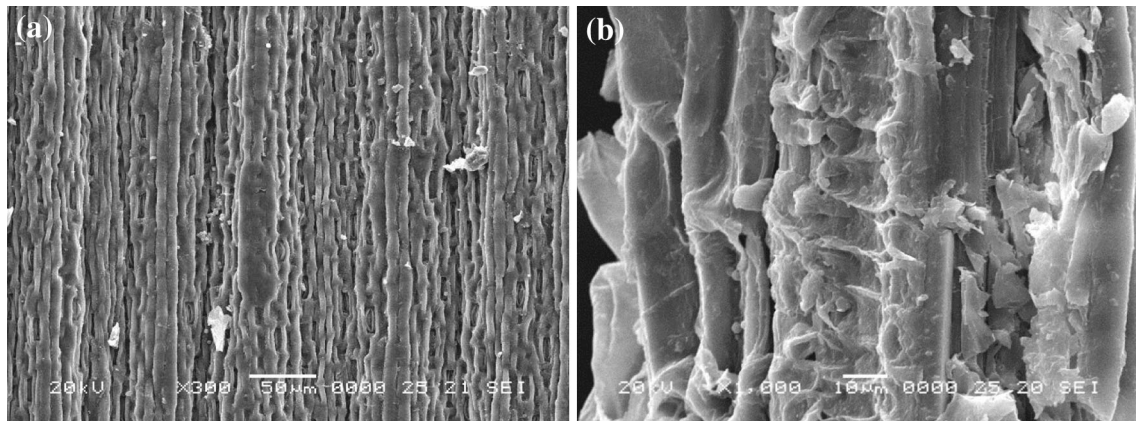


Fig. 2 The morphology of raw cattail leave **a** $\times 300$, **b** $\times 1,000$ magnification

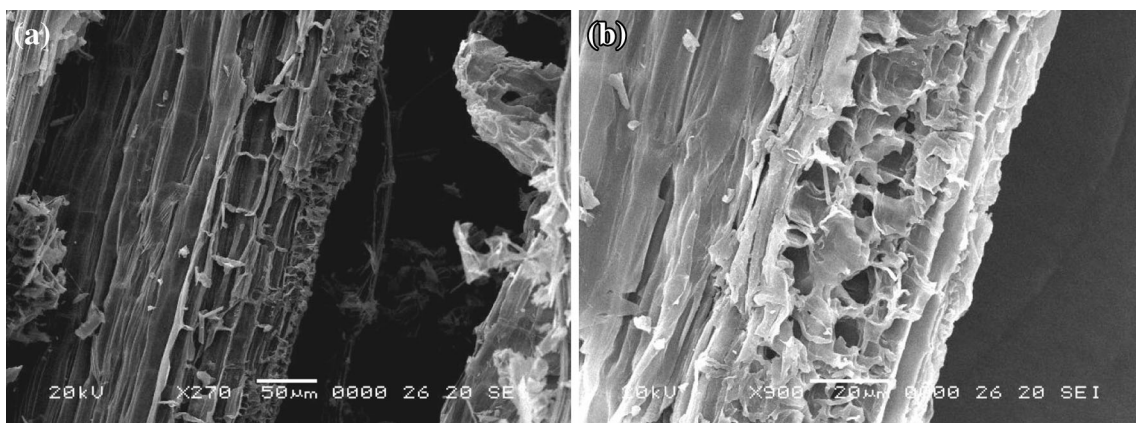


Fig. 3 The morphology of AC1 **a** $\times 270$, **b** $\times 900$ magnification

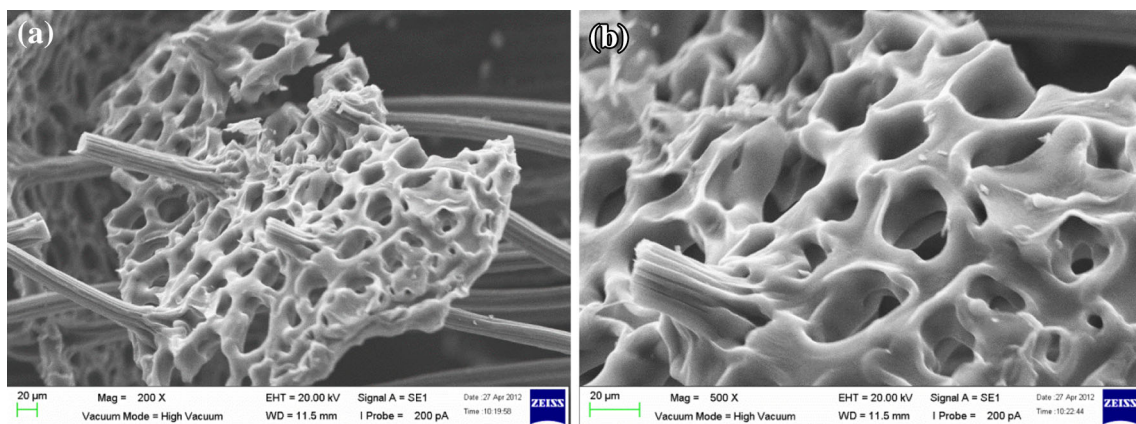


Fig. 4 The morphology of AC2 **a** $\times 200$, **b** $\times 500$ magnification

to be 7.946 mg/g. Figure 7 shows that different concentrations of H_3PO_4 AC prepared from cattail leaves were analyzed in 4 ppm Pb(II) aqueous solution with respect to the contact time. All the prepared AC showed the similar trend of adsorption rate with no significant effect towards

the contact time within the first 5 min, and showed a rapid adsorption. Then, the subsequent time showed a slow adsorption process. The highest percentage removal efficiency for AC1, AC3 and AC4 was found to be 37.4, 92.3, and 91.9 %, respectively. The lower percentage removal

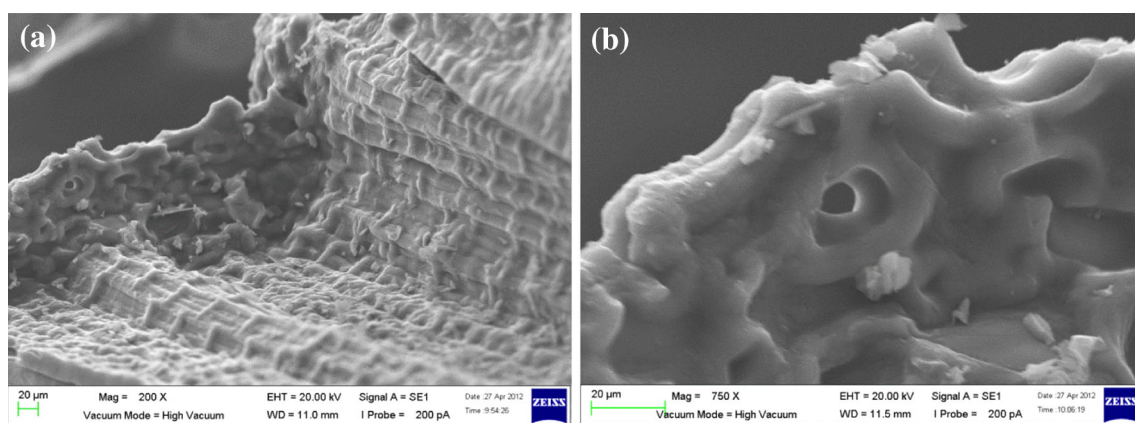


Fig. 5 The morphology of AC3 **a** $\times 200$, **b** $\times 750$ magnification

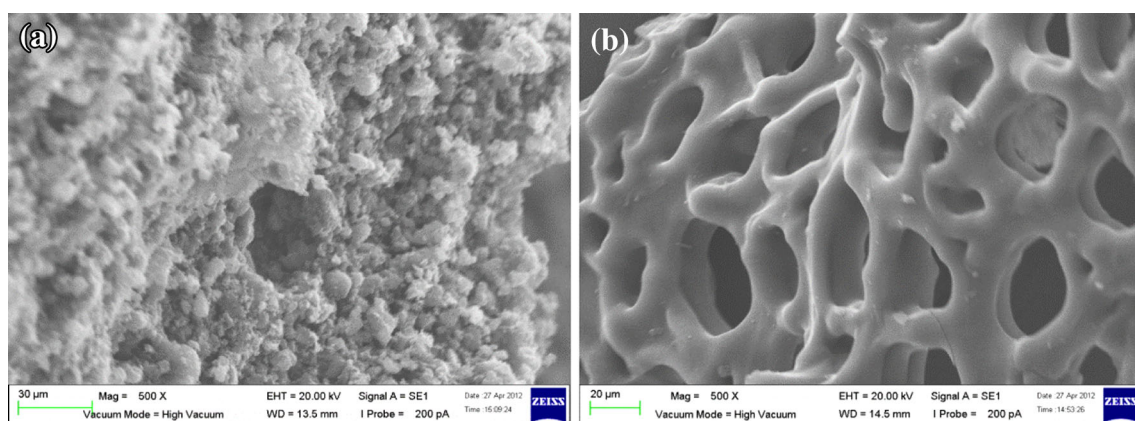


Fig. 6 The morphology of AC4 **a** $\times 500$, **b** $\times 500$ magnification

Table 3 Porous and surface properties of AC

Description	Langmuir	Brunauer–Emmett–Teller (BET)	Mesopores Barrett–Joyner–Halenda (BJH)	Mesopores (Cranston and Inkley)	Mesopores (Dollimore and Heal)	Micropores Horvath and Kawazoe	Micropores (Saito and Foley)
Surface area (m^2/g)	1238.60	966.74	–	–	–	–	–
Cumulative pore area (m^2/g)	–	–	12.783	12.795	12.783	1090.7	578.02
Pore volume (cm^3/g)	284.55	222.1	–	–	–	–	–
Cumulative pore volume (cm^3/g)	–	–	0.0462	0.0462	0.0462	0.4491	0.4491

efficiency from these activated carbons might be due to the saturation of active site on the surface of AC.

Effect of initial concentration on Pb(II) adsorption

Figure 8 shows the absorbance value of Pb(II) as a function of time for a range of Pb(II) concentrations and the

experimental data. The effect of initial concentration is more efficient at low Pb(II) concentration [30]. This is because at low Pb(II) concentration, the ratio of the adsorption site to the total mean ions in the solution is high and hence all the Pb(II) may interact with the adsorbent and finally removed from the solution. In accordance with this result, the optimum concentration of Pb(II) to obtain a

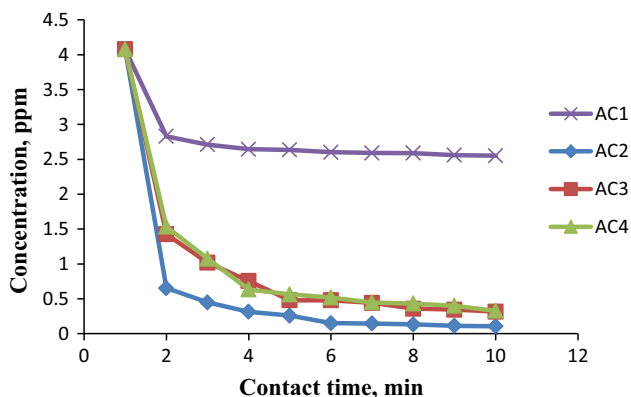


Fig. 7 Effect of different contact time on Pb(II) adsorption onto AC1, AC2, AC3 and AC4: 200 mL of 4 ppm

higher adsorption capacity may be considered about 1–4 ppm.

Effect of dosage of adsorbent on Pb(II) adsorption

The highest percentage of Pb(II) removal is found with AC2. The effect of the adsorbent dosage on the removal of Pb(II) from aqueous solution is investigated by varying the dosage of the adsorbent as shown in the Fig. 9. It was expected an increase in the percentage removal when the adsorbent dose per 200 mL of solution was increased from 0.1 to 0.5 g. This is because there are more adsorption sites for the adsorbate to be occupied with the increase of the adsorbent dosage. Therefore, as dosage of adsorbent increases, the competition for bonding sites between molecules of the adsorbate and adsorbent decreases. The experiment data proved that the use of cattail AC as adsorbent depends on its dosage in aqueous solution. Similar result was found on the effect of dosage of adsorbent on Pb(II) adsorption using tea waste [30].

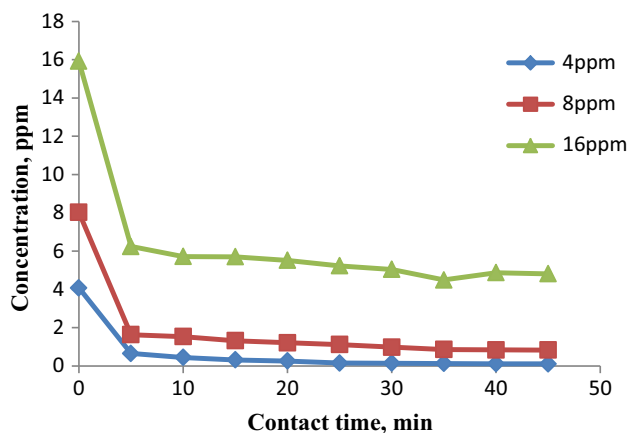


Fig. 8 Effect of different initial concentration on Pb(II) adsorption onto AC2: 200 mL of 4 ppm

Adsorption kinetics

The study of the adsorption kinetics is important to evaluate the mechanism and efficiency of adsorption process. The kinetics of Pb(II) by prepared AC were analyzed using pseudo-first-order and pseudo-second-order kinetic models (Figs. 10, 11). The data for adsorption kinetics are shown in Table 4. The adsorption of AC2 was best fitted to pseudo-second-order kinetic model as indicated by the high R^2 value of 0.9999 (Fig. 11) compared to pseudo-first-order kinetic model (Fig. 10, $R^2 = 0.9626$). The confirmation of pseudo-second-order kinetics suggests that adsorption of Pb(II) by AC2 is due to chemisorption process. The equilibrium sorption capacity, q_e , only needs to be known and the first-order model fits well for the whole range of contact times [31]. This is because in chemisorption process it tends to become slow which causes the amount sorbed to remain significantly smaller than the equilibrium value. Thus, the pseudo-first-order model did not precisely represent the adsorption kinetics in this study because q_e is usually obtained via trial and error method.

Pseudo-second-order is more likely to predict the behavior of whole range of contact times in adsorption process which is in agreement with chemisorption being the rate determining step [31]. Chemisorption process involved a sharing of electron between the adsorbate and the surface of adsorbent. Although it might be followed by additional layers of physically adsorbed molecules, it is restricted to just one layer of molecules on the surface in chemisorption process [32]. Similar adsorption kinetic results have also been obtained from biosorption of Pb(II) by cattail leaves and tea waste [29, 30].

Adsorption isotherm

Adsorption isotherms are used to calculate the theoretical adsorption capacity of an adsorbent. The Langmuir and Freundlich models used for this present study are the most

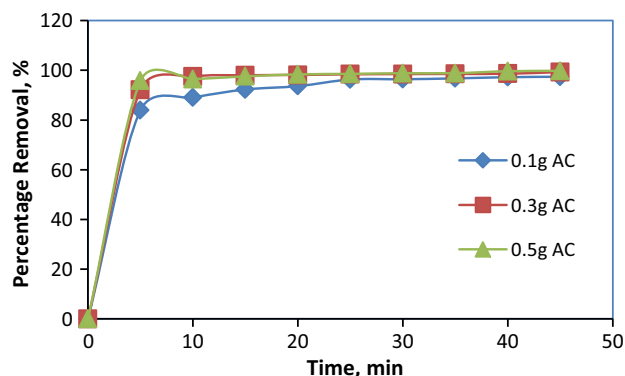


Fig. 9 Effect of different dosage of adsorbent on Pb(II) adsorption onto AC2: 200 mL of 4 ppm

Fig. 10 Pseudo-first-order kinetics of Pb(II) on AC2: 0.1 g of AC2 mixed with 200 mL of solution

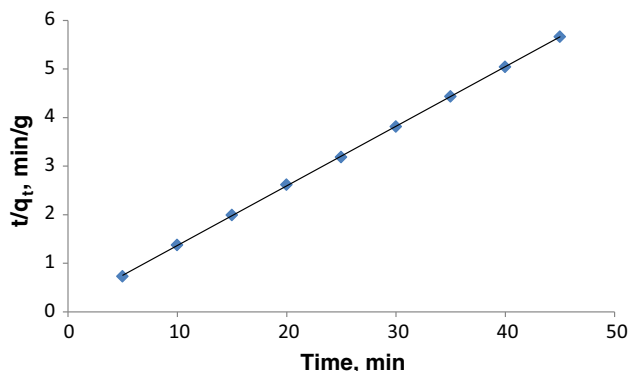
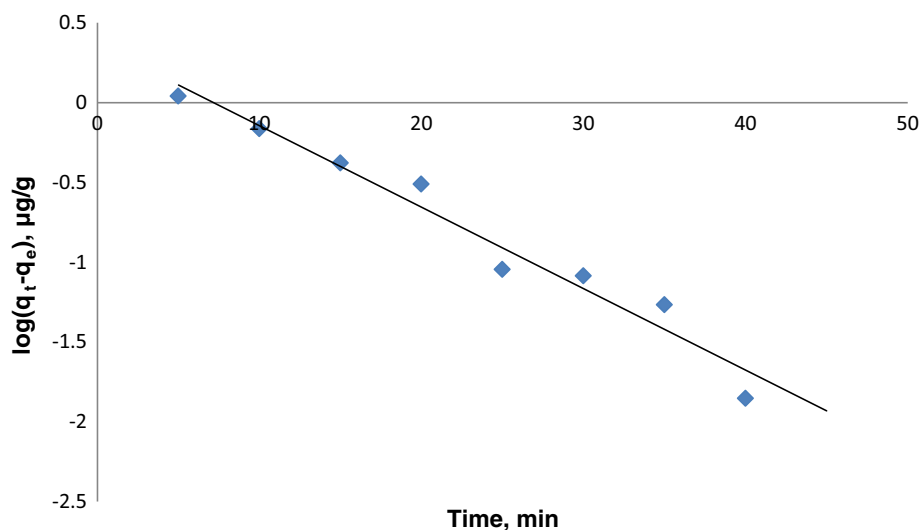


Fig. 11 Pseudo-second-order kinetics of Pb(II) on AC2: 0.1 g of AC2 mixed with 200 mL of solution

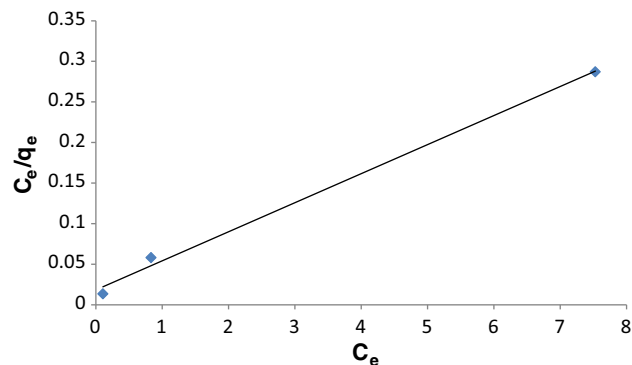


Fig. 12 Langmuir adsorption isotherm for Pb(II) onto AC2

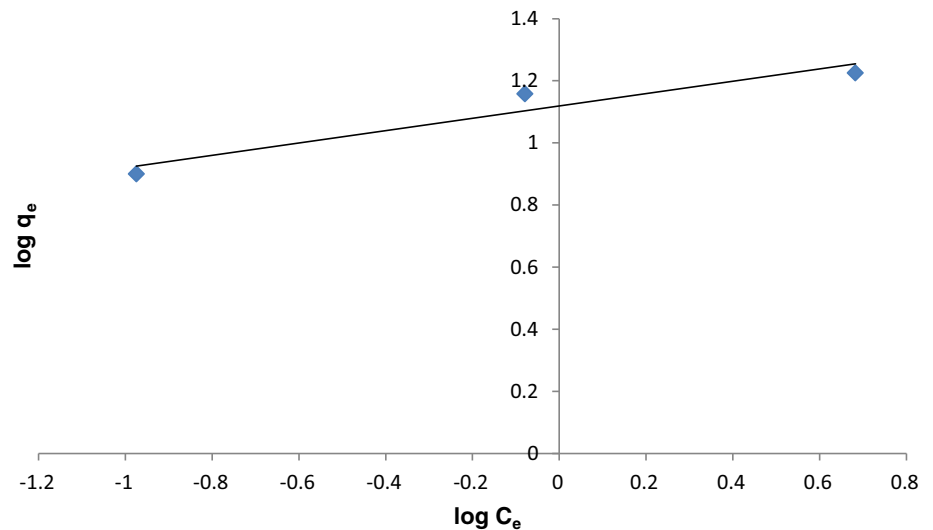
common models that are applied for aqueous solutions. Sorption can be physisorption or chemisorption to describe the metallic or organic materials that are attached to an adsorbent. The equilibrium is achieved when the capacity of the adsorbent is saturated, thus the rate of adsorption equals to the rate of desorption [33]. Normally, the

concentration of adsorbate remaining in the wastewater at the equilibrium depends on the type of AC and type of concentration [34, 35]. Figures 12 and 13 show the Langmuir and Freundlich models of AC2, respectively. Data of Langmuir and Freundlich isotherm parameters for adsorption of Pb(II) onto AC samples clearly show that all the chemically prepared AC showed higher regression

Table 4 Pseudo-first and second-order kinetic parameters for adsorption of Pb(II) onto AC2

Time (min)	c_o	c_e	c_t	q_t	q_e	$\text{Log}(q_e - q_t)$	t/q_t
5	4.079	0.106	0.654	6.85	7.946	0.039811	0.729927
10	4.079	0.106	0.449	7.26	7.946	-0.16368	1.37741
15	4.079	0.106	0.315	7.528	7.946	-0.37882	1.992561
20	4.079	0.106	0.260	7.638	7.946	-0.51145	2.618487
25	4.079	0.106	0.151	7.856	7.946	-1.04576	3.184852
30	4.079	0.106	0.147	7.864	7.946	-1.08619	3.814852
35	4.079	0.106	0.133	7.892	7.946	-1.26761	4.434871
40	4.079	0.106	0.113	7.932	7.946	-1.85387	5.042864
45	4.079	0.106	0.103	7.946	7.946	-	5.663227



Fig. 13 Freundlich adsorption isotherm for Pb(II) onto AC2**Table 5** Efforts by researchers to prepare AC using H₃PO₄ activation with reference to the precursors, experiment conditions and product quality

References	Precursors	Experimental condition	Product quality
[15]	Cotton stalk	Dried, crushed cotton stalks were impregnated with varying concentrations of H ₃ PO ₄ (20–85 wt%), dried at 383 K and carbonized at 773 K for 2 h	773 K is suitable for the production of AC from cotton stalks by pre-impregnation with H ₃ PO ₄ (30–65 wt%). Carbons with well-developed mesoporosity and high surface area (1,032 m ² /g). A lower temperature of 673 K produces a carbon with relatively lower surface area and porosity
[36]	Grain sorghum	Nitrogen atmosphere; two-stage and three-stage; in two-stage pre-drying at 100 °C followed by activation at 450–700 °C. In three-stage process carbonization at 300 °C for 15 min followed by impregnation and activation temperature 400–600 °C	The surface area increased from 156 to 528 m ² /g with an increase of acid concentration from 10 to 35 %. The surface area increased from 975 to 1,522 m ² /g when the activation temperature was elevated from 400 to 500 °C
[26]	Date pits	The raw material was impregnated with increasing concentrations of H ₃ PO ₄ (30–70 vol%) followed by pyrolysis at 300, 500 or 700 °C. Texture characteristics of the products were determined by adsorption of N ₂ at 77 K, as well as iodine, phenol, and methylene blue values	Low porosity carbons obtained at 300 °C show good capacity to remove substrates from solution (iodine, phenol, MB). The optimum activant concentration, to get the best adsorbing carbons, lies within 50 and 60 wt% which corresponds to an acid to precursor weight ratio of 1.20–1.44
[37]	Bamboo	AC was produced using H ₃ PO ₄ treatment of the waste bamboo scaffolding and activated at either 400 or 60 °C. The effect of acid to bamboo ratio (X _p) up to 2.4 has been studied. Firstly, the mixtures were heated at 150 °C for 2 h and then heated to either 400 or 600 °C in a furnace under flowing nitrogen for 4 h	The BET surface area increased with increasing X _p and activating temperature. High surface area with high pore volume was produced at 600 °C with acid to bamboo mass ratio of 2.41. Both surface area and porosity were affected by the activation temperature and acid to bamboo ratio
This work	Cattail leaves	AC was prepared from cattail leaves using physical and chemical activation of H ₃ PO ₄ , as dehydrating agent. A two-stage process was used, i.e., semi-carbonization stage at 200 °C for 15 min as first stage followed by second-stage activation, at 500 °C for 45 min	The best condition in AC production was AC2 with 2 M of H ₃ PO ₄ . AC2 has the highest removal efficiency, 97.4 % in 4 ppm concentration of Pb(II) and percentage yield of 62.73 %. The maximum BET surface area was found to be around 1,238 m ² /g and the maximum adsorption capacity was 7.95 mg/g

coefficient value in the Langmuir isotherm compared to Freundlich isotherm. But AC2 was best fitted to Langmuir isotherm with the highest regression coefficient ($R^2 = 0.9999$) as compared to other prepared AC. The

Langmuir isotherm was based on three assumptions: (a) the adsorption is a monolayer adsorption, and only one layer of molecules is attached to the surface; (b) the surface has specific number of sites on the adsorbent which are



occupied by the adsorbate in the solution; (c) the adsorbate is strongly attached to the surface of the adsorbent. This isotherm is based on the view that every adsorption site is equivalent and independent; the ability of a molecule to bind is independent of whether or not neighboring sites are occupied. However, AC1 which is a physically prepared AC fits better in the Freundlich isotherm. It is due to its sorption ability on heterogeneous surface, hence the uptake of Pb(II) may involve multi-molecular layer adsorption [35]. Table 5 shows the literature values of previous studies of AC using H₃PO₄ activation for comparison.

Conclusions

This study shows that cattail leaves which had no economic value are suitable for the production of AC as adsorbent. It produces a high percentage yield and gave an acceptable range of moisture and ash content for producing good adsorbent. The washing process played a crucial role in the porosity development because some of the pores might be clogged with H₃PO₄ molecule. The morphology studies indicated that the prepared AC had clear burnout pore with honey comb-like structure. FTIR spectra showed that AC were occupied by several functional groups, such as C–O, C=O, O–H, C=C. This study also shows that AC2 produced from two-stage activation with impregnation concentration of 2 M H₃PO₄ yielded the best performance AC with highest percentage removal of Pb(II), 97.4 %. The Langmuir isotherm was the best to describe the Pb(II) adsorption isotherm for AC production with a correlation coefficient ($R^2 = 0.9999$). Besides that, the kinetic data best fitted into pseudo-second-order rate equation with $R^2 = 0.9999$. The maximum adsorption capacity was found to be 7.95 mg/g.

Author contribution WSY carried out the experiments and analysis. SMA and CGJ participated in interpretation of results and drafted the manuscripts. WMABWD and DK participated in the critical review and also did the revision of the manuscript. All authors read and approved the final manuscript.

Acknowledgments This work was fully supported by the Centre of Research & Innovation, Universiti Malaysia Sabah (Grant No. SBK0058-SG-2013) and is gratefully acknowledged.

Conflict of interest The authors declare that they have no competing interests.

Open Access This article is distributed under the terms of the Creative Commons Attribution License which permits any use, distribution, and reproduction in any medium, provided the original author(s) and the source are credited.

References

1. Attia AA, Girgis BS, Fathy NA (2008) Removal of methylene blue by carbons derived from peach stones by H₃PO₄ activation: batch and column studies. *Dyes Pigments* 76:282–289
2. Tseng ML, Lin YH, Chiu ASF (2009) Fuzzy AHP-based study of cleaner production implementation in Taiwan PWB manufacturer. *J Clean Prod* 17:1249–1256
3. Tseng ML (2010) An assessment of cause and effect decision-making model for firm environmental knowledge management capacities in uncertainty. *Environ Monit Assess* 161:549–564
4. Hu ZH, Yu HQ (2006) Anaerobic digestion of cattail by rumen cultures. *Waste Manage* 26:1222–1228
5. Hansen D, Duda PJ, Zayed A, Terry N (1998) Selenium removal by constructed wetlands: role of biological volatilization. *Environ Sci Technol* 32:591–597
6. Bankston JL, Sola DL, Komor AT, Dwyer DF (2002) Degradation of trichloroethylene in wetland microcosms containing broad-leaves cattail and eastern cottonwood. *Water Res* 36:1539–1546
7. Ciria MP, Solano ML, Soriano PT (2005) Role of macrophyte *Typha latifolia* in a constructed wetland for wastewater treatment and assessment of its potential as a biomass fuel. *Biosyst Eng* 92:535–544
8. Breen PF (1990) A mass balance method for assessing the potential of artificial wetlands for wastewater treatment. *Water Res* 24:689–697
9. Chen TY, Kao CM, Yeh TY, Chien HY, Chao AC (2006) Application of a constructed wetland for industrial wastewater treatment: a pilot-scale study. *Chemosphere* 64:497–502
10. Heritage A, Pistillo P, Sharma KP, Lantzeke IR (1995) Treatment of primary-settled urban sewage in pilot-scale vertical flow wetland filters: comparison of four emergence macrophyte species over a 12 month period. *Water Sci Technol* 32:295–304
11. Zhang J, Shi QQ, Zhang CL, Xu JT, Zhai B, Zhang B (2008) Adsorption of neutral red onto Mn-impregnated activated carbons prepared from typha orientalis. *Bioresour Technol*. 99:8974–8980
12. Srinivasakannan C, Abu Bakar MZ (2004) Production of activated carbon from rubber wood sawdust. *Biomass Bioenerg*. 27:89–96
13. Joseph CG, Frankie Y (2008) Textural and chemical characterization of activated carbon prepared from rice husk (*oryza sativa*) using a two-stage activation process. *J Eng Sci Technol* 3:234–242
14. SIRIM (1984) Specification of powdered activated carbon MS873: 1984. Standardization and Industrial Research Institute Malaysia, Kuala Lumpur
15. Girgis BS, Ishak MF (1999) Activated carbon from cotton stalk by impregnation with phosphorus acid. *Mater Lett* 39:107–114
16. Liu QS, Zheng T, Wang P, Guo L (2009) Preparation and characterization of activated carbon from bamboo by microwave-induced phosphoric acid activation. *Ind Crop Prod* 31:233–238
17. Laszlo K, Bota A, Nagy LG (1996) Characterization of activated carbon from waste material by adsorption from aqueous solution. *Carbon* 35:593–598
18. Yacob AR, Al Swaidan AM (2012) Phosphoric acid effect on prepared activated carbon from Saudi Arabia's date frond waste. *Appl Mech Mater* 110–116:2124–2130
19. Zhou L, Li M, Sun Y, Zhou Y (2001) Effect of moisture in microporous activated carbon on methane. *Carbon* 39:773–776
20. Shi QQ, Zhang J, Zhang CL, Li C, Zhang B, Hu W, Xu JT, Zhao R (2010) Preparation of activated carbon from cattail and its application for dyes removal. *J Environ Sci* 22:91–97
21. Ren L, Zhang J, Li Y, Zhang CL (2011) Preparation and evaluation of cattail fiber-based activated carbon for 2,4-dichlorophenol and 2,4,6-trichlorophenol removal. *Chem Eng J* 168:553–561

22. Guo Y, Rockstraw DA (2006) Physical and chemical properties of carbon syntheses from xylan, cellulose, and Kraft lignin by H_3PO_4 activation. *Carbon* 44:1464–1475
23. Jagtoyen M, Derbyshire F (1993) Some consideration of the origins of porosity in carbons from chemically activated wood. *Carbon* 31:1185–1192
24. Puziy AM, Poddubnaya OL, Martinez-Alonso A, Suarez-Garcia F, Tascon JMD (2002) Synthetic carbons activated with phosphoric acid: surface chemistry and ion binding properties. *Carbon* 40:1493–1505
25. Jankowska H, Swiatkowski A, Choma J (1991) Active carbon. Ellis Horwood Limited, Poland
26. Girgis BS, El-Hendawy AN (2002) Porosity development in activated carbons obtained from date pits under chemical activation with phosphoric acid. *Microporous Mesoporous Mater* 52:105–117
27. Molina-Sabio M, Rodriguez-Reinoso F (2004) Role of chemical activation in the development of carbon porosity. *Colloids Surf A* 241:15–25
28. El-Hendawy ANA, Alexander AJ, Andrews RJ, Forrest G (2008) Effect of activation schemes on porous, surface and thermal properties of activated carbon prepared from cotton stalks. *J Anal Appl Pyrol* 82:272–278
29. Liew SYL, Joseph CG, How SE (2011) Biosorption of lead contaminated wastewater using cattails (*Typha angustifolia*) leaves: kinetic studies. *J Serb Chem Soc* 76:1037–1047
30. Amarasinghe BMWPK, Williams RA (2007) Tea waste as low cost adsorbent for the removal of Cu and Pb from wastewater. *Chem Eng J* 132:299–309
31. Ho YS, McKay GA (1998) A comparison of chemisorption kinetic models applied to pollutant removal on various sorbents. *T I Chem Eng Lond* 76:332–340
32. El Qada EN, Allen SJ, Walker GM (2006) Adsorption of methylene blue onto activated carbon produced from steam activated bituminous coal: a study of equilibrium adsorption isotherm. *Chem Eng J* 124:103–110
33. Payne BK, Abdel-Fattah MT (2004) Adsorption of divalent lead ions by zeolites and activated carbon: effects of pH, temperature, and ionic strength. *J Environ Sci Heal A* 39:2275–2291
34. Anisuzzaman SM, Bono A, Krishnaiah D, Tan YZ (2014) A study on dynamic simulation of phenol adsorption in activated carbon packed bed column. *J King Saud Univ Eng Sci* (in press)
35. Krishnaiah D, Anisuzzaman SM, Bono A, Sarbatly R (2013) Adsorption of 2,4,6-trichlorophenol (TCP) onto activated carbon. *J King Saud Univ Sci* 25:251–255
36. Diao Y, Walawender WP, Fan LT (2002) Activated carbons prepared from phosphoric acid activation of grain sorghum. *Bioresour Technol* 81:45–52
37. Chan LS, Cheung WH, Allen SJ, McKay G (2009) Separation of acid-dyes mixture by bamboo derived active carbon. *Sep Purif Technol* 67:166–172

